THE JOURNAL OF PHYSICAL CHEMISTRY B

Article

pubs.acs.org/JPCB

Synthesis of Electromagnetic Functionalized Fe_3O_4 Microspheres/Polyaniline Composites by Two-Step Oxidative Polymerization

Chenkui Cui,[†] Yunchen Du,*[,†] Tianhao Li,[†] Xiaoying Zheng,[†] Xiaohong Wang,[‡] Xijiang Han,[†] and Ping Xu*[,†]

[†]Chemistry Laboratory Center, Department of Chemistry, Harbin Institute of Technology, Harbin 150001, China

[‡]Beijing Institute of Aeronautical Materials, Beijing 100095, China

Supporting Information

ABSTRACT: Composites consisting of Fe_3O_4 microspheres (FMS) and polyaniline (PANI), FMS/PANI, have been successfully prepared through a two-step oxidative polymerization of aniline monomers in the presence of Fe_3O_4 microspheres. In our two-step polymerization technique, Fe^{3+} and ammonium persulfate (APS) are used as the oxidants in each step. It is discovered that the two-step oxidative process plays a dominant role in the morphology of these composites: aniline oligomers oxidized by Fe^{3+} are mainly produced in the first stage, and "egg-like" PANI aggregates are obtained in the second stage. It can be found that embedding Fe_3O_4 microspheres in the polymer matrixes will not only modulate the complex permittivity but also produce magnetic resonance and loss in the composites. Therefore, the characteristic impedance and reflection loss of these composites are greatly improved. Especially, the composite with equal amount of FMS and PANI, FMS/$PANI_{50}$, displays very strong reflection loss over a wide frequency range that can be manipulated by the absorber thickness. More importantly, the composites prepared from the two-step chemical oxidative polymerization using hierarchical magnetic materials have better microwave absorption and environmental stability as compared with those composites from Fe_3O_4 nanoparticles, one-step oxidative polymerization, and physical mixture. We believe the two-step oxidative polymerization technique can be a novel route for the design and preparation of lightweight and highly effective microwave absorbers in the future.

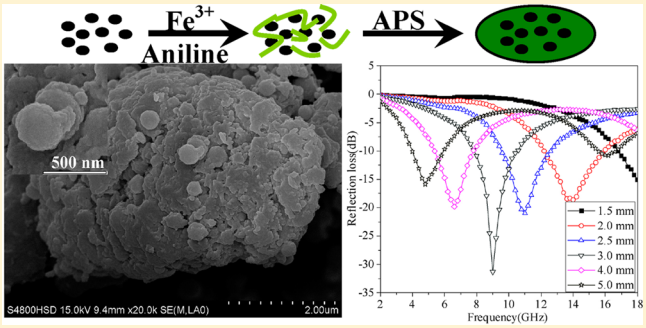

1. INTRODUCTION

With the expanded applications of electromagnetic waves in civil and military fields, it becomes urgent to design and fabricate microwave absorbers to eliminate or at least decrease the ensuing problems in electromagnetic interference, human health, environmental pollution, etc. Among many new microwave absorbers, electrically conductive polymers such as polyaniline (PANI) and polypyrrole (PPy) have been considered as promising candidates as microwave absorbers due to their high conductivity, low density, ease of preparation, and good environmental stability.[1,2] However, pure conductive polymers have relatively high complex permittivity ($\varepsilon = \varepsilon' + j\varepsilon''$) and quite low complex permeability ($\mu = \mu' + j\mu''$), resulting in poor matching between complex permittivity and complex permeability, which deviates from the zero-reflection condition at the surface of the materials.[3] Therefore, conducting polymers themselves cannot produce considerable attenuation of incident electromagnetic waves.[4−7] Interestingly, recent works have indicated that embedding magnetic particles, including Ni,[4,8] γ-Fe_2O_3,[9] $BaFe_{12}O_{19}$,[10−12] and carbonyl iron powders,[13] into conductive polymer matrixes can be an effective way to optimize the electromagnetic parameters and improve microwave absorbing properties.

As a conventional microwave absorbing material, Fe_3O_4 has also been frequently used as a promoter for microwave absorption enhancement of conductive polymers due to its excellent magnetic properties and easy preparation.[13−18] For example, He et al. prepared Fe_3O_4 nanoparticles/PANI composite by chemical oxidative polymerization, and the resultant product showed good microwave absorption in the 2−18 GHz frequency range;[13] Phang et al. also obtained composites composed of Fe_3O_4 nanoparticles and PANI, whereas the assistance of TiO_2 and $FeCl_3$ treatment were necessary for the enhanced microwave absorption;[15,16] Yang et al. and Li et al. designed hollow Fe_3O_4/PANI microspheres and core−shell Fe_3O_4/PPy, respectively, to produce effective loss for incident electromagnetic waves.[17,18] However, it is very important to note that almost all composites are fabricated from Fe_3O_4 nanoparticles (ca. 10−100 nm),[13−18] which usually show very limited permeability in the gigahertz range induced by Snoek's limit;[19] thus the enhancement of microwave absorption of these composites is still mainly from dielectric

Received: March 13, 2012
Revised: July 9, 2012
Published: July 16, 2012

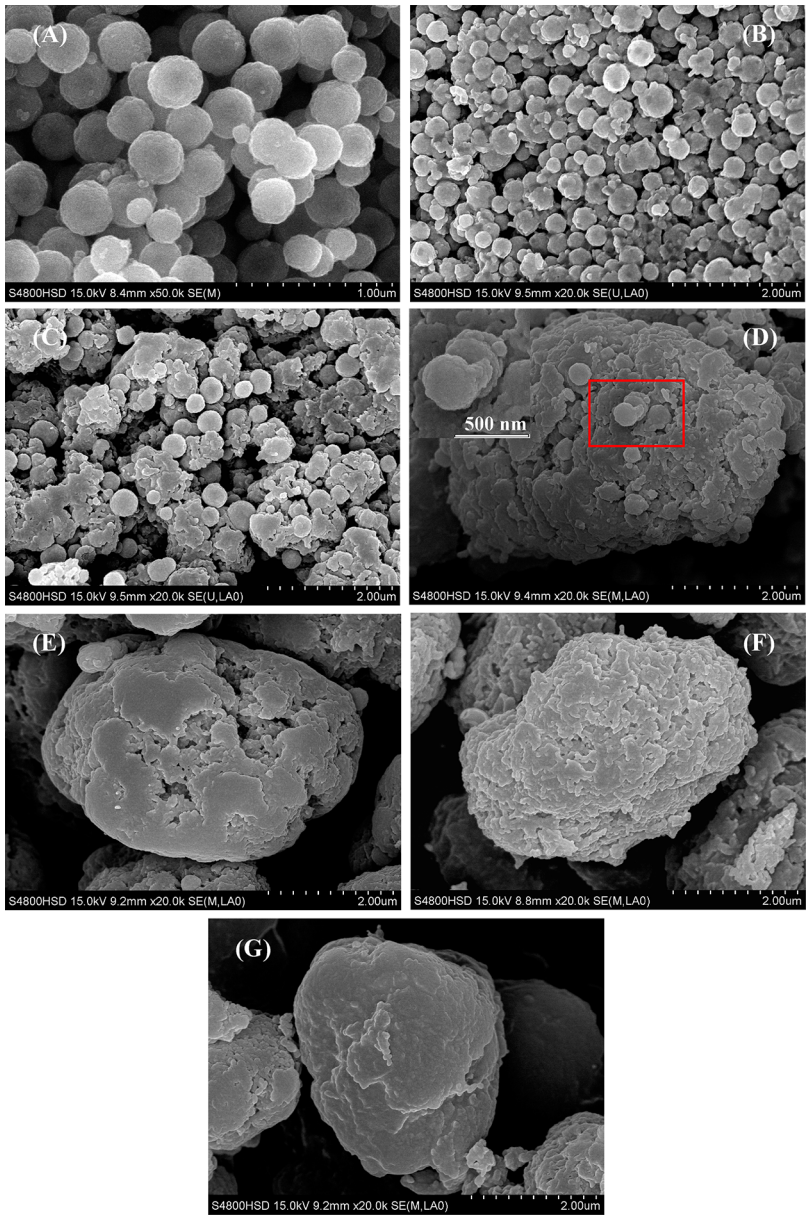

Figure 1. SEM images of FMS/$PANI_0$ (A), FMS/$PANI_{10}$ (B), FMS/$PANI_{30}$ (C), FMS/$PANI_{50}$ (D), FMS/$PANI_{70}$ (E), FMS/$PANI_{90}$ (F), and FMS/$PANI_{100}$ (G).

loss rather than a combination of dielectric and magnetic loss in most cases.[13,18] More recently, some unique aggregates of Fe_3O_4 nanoparicles, such as urchin-like structure,[20] loose microspheres,[21,22] hollow nanospheres,[23] and dendrite-like structure,[24] have been constructed to break through Snoek's limit and produce characteristic magnetic loss for gigahertz electromagnetic waves. Therefore, it should be promising and meaningful to enhance magnetic loss and further improve microwave absorbing properties of Fe_3O_4/conductive polymers composites by embedding above-mentioned aggregates.

In this paper, we demonstrated the synthesis of Fe_3O_4 microspheres/PANI (FMS/PANI) composites by a two-step chemical oxidation polymerization method. The morphology evolution and microwave absorption of these composites with different contents of Fe_3O_4 microspheres were investigated. Compared with those composites prepared from one-step oxidation and physical mixture, FMS/PANI samples herein show better microwave absorbing properties. Especially, the composite with equal amounts of FMS and PANI, FMS/$PANI_{50}$, shows reflection loss exceeding −10 dB in the range 4−18 GHz by manipulating the thickness from 1.5 to 5.0 mm and a maximum reflection loss can reach −31.3 dB at 9 GHz with a thickness of 3.0 mm.

2. EXPERIMENTAL SECTION

2.1. Synthesis of Fe_3O_4 Microspheres. Fe_3O_4 microspheres were prepared according to a previous literature.[25] Briefly, 5.40 g of $FeCl_3 \cdot 6H_2O$ were dissolved in 200 mL of ethylene glycol under magnetic stirring, and then 14.4 g of sodium acetate was added. The obtained homogeneous yellow solution was transferred into a Teflon-lined stainless-steel autoclave and sealed to heat at 200 °C for 8 h. The obtained black magnetite particles were washed with distilled water and absolute ethanol to remove the residues, and then dried at 50 °C.

dx.doi.org/10.1021/jp3024099 | J. Phys. Chem. B 2012, 116, 9523−9531

2.2. Synthesis of Fe_3O_4 Microspheres/Polyaniline Composites (FMS/PANI). Required amounts of Fe_3O_4 microspheres were dispersed into 100 mL of stock solution containing 0.25 M $FeCl_3$ and 0.02 M HCl, and then aniline monomer was added. The solution was mechanically stirred in an ice−water bath for 10 h before adding precooled ammonium persulfate (APS) aqueous solution for oxidative polymerization for another 12 h. The precipitated powder was filtrated and washed with distilled water and ethanol until the filtrate became colorless and then dried in a vacuum drying cabinet at 70 °C. Throughout the experiment, the total mass of Fe_3O_4 microspheres and aniline monomer was 2.0 g, and the molar ratios of aniline to APS ((An)/(APS)) were fixed at 0.4. To confirm that PANI was sufficiently doped with HCl, the dried powder could be redispersed in 0.1 M HCl under ultrasonication for 30 min and collected by filtration and drying again. The final composites were denoted as FMS/$PANI_x$, where x suggested the weight percent of (aniline monomer)/(Fe_3O_4 + (aniline monomer)) in initial solution. For comparison, pure polyaniline (FMS/$PANI_{100}$) was prepared in the absence of Fe_3O_4 microspheres with the same procedures.

2.3. Synthesis of One-Step Oxidized Fe_3O_4 Microspheres/Polyaniline Composites (OO-FMS/PANI), Fe_3O_4 Nanoparticles/Polyaniline Composites (FNP/PANI), and Physically Mixed Fe_3O_4 Microspheres/Polyaniline Composites (PM-FMS/PANI). In the synthesis of OO-FMS/$PANI_{50}$, 1.0 g of Fe_3O_4 microspheres and 1.0 g of aniline monomer were dispersed into 100 mL of 0.02 M HCl solution and the mixture was stirred in an ice−water bath for 1 h. After 10 mL of APS solution was added, the mixture was continuously stirred for 22 h. The obtained powder was then treated by the same process with that of FMS/PANI.

FNP/$PANI_{50}$ was prepared following the same process with that of FMS-$PANI_{50}$, except that 1.0 g of Fe_3O_4 nanoparticles (prepared according to previous literature[26]) was used to replace 1.0 g of Fe_3O_4 microspheres.

For PM-FMS/PANI, 1.0 g of Fe_3O_4 microspheres and 0.7 g of PANI prepared by two-step oxidation were thoroughly ground in an agate mortar for 25−30 min at room temperature.

2.4. Characterization. Powder X-ray diffraction (XRD) data were recorded on a XRD-6000 X-ray diffractometer (Shimadzu) with a Cu Kα radiation source (40.0 kV, 30.0 mA). Scanning electron microscope (SEM) images were obtained on the S-4800 (Hitachi), and the samples were mounted on aluminum studs by using adhesive graphite tape and sputter-coated with gold before analysis. The thermogravimetric (TG) analysis was carried out on a SETSYS Evolution TGA (Setaram) in the temperature range of room temperature to 800 °C using a heating rate of 10 °C min^{-1}. FT-IR spectroscopy was carried out on a Nicolet Avatar 360 FT-IR spectrometric analyzer with KBr pellets. UV/vis spectra were recorded on a PUXI TU-1901 spectrophotometer by dissolving FMS/PANI samples in *N*-methylpyrrolidone (ca. 0.2 mg/mL). X-ray photoelectron spectroscopy (XPS) was recorded at room temperature in a PHI 5700 ESCA system. A HP-5783E vector network analyzer was applied to determine the relative permeability and permittivity in the frequency range 2−18 GHz for the calculation of reflection loss. A sample containing 50 wt % obtained composites was pressed into a ring with an outer diameter of 7 mm, an inner diameter of 3 mm, and a thickness of 2 mm for microwave measurement in which paraffin wax was used as the binder.

3. RESULTS AND DISCUSSION

Figure 1 shows the morphology evolution of FMS/PANI composites from different mass contents of PANI. In the case of Fe_3O_4 microspheres (FMS/$PANI_0$) (Figure 1A), it can be found that the sample is fully composed of spherical particles with an average diameter of about 300 nm, which is quite coincident with the previous report.[25] With the increase in the content of the organic phase, some disordered PANI particles appear around Fe_3O_4 microspheres and the surfaces of some microspheres become rough (Figure 1B,C), indicating the beginning of coating process of PANI, but Fe_3O_4 microspheres are not fully coated due to the low content of PANI. When an equal amount of aniline monomer (FMS/$PANI_{50}$) is used, bulky aggregates of PANI are formed on Fe_3O_4 microspheres (Figure 1D), forming an "egg-like" structure that is about 5 μm in length and 3 μm in width. Although several isolated Fe_3O_4 microspheres located at the external surface of bulky aggregates can still be observed, the rough surface of these isolated microspheres revealed by a high-resolution image (Figure 1D, inset) suggests that they have also been coated by PANI. Further increasing the content of PANI, no Fe_3O_4 microspheres can be seen, and the aggregates display a continuous growth and decreased defects on the surface (Figure 1E,F). Pure PANI exhibits a similar microstrucure with a smooth external surface (Figure 1G). It is generally accepted that the morphology of PANI is easily directed by adding some seed templates, such as particulate, fibers, and nano/microspheres,[10,27,28] into the polymerization system of aniline. However, the presence of Fe_3O_4 microspheres herein does not seem to work. As comparisons, FNP/$PANI_{50}$ from Fe_3O_4 nanoparticles and two-step oxidation exhibits microstructure quite similar to that of FMS/$PANI_{50}$, whereas OO-FMS/$PANI_{50}$ from one-step oxidation by APS shows disordered microstructure with irregular aggregates and coated microspheres (Figure S1, Supporting Information). Thus, the unique "egg-like" structure in FMS/PANI composites should be due to the two-step oxidation−polymerization system. On the basis of the results of SEM, we propose a possible mechanism on the growth of FMS/PANI composites, as shown in Figure 2.

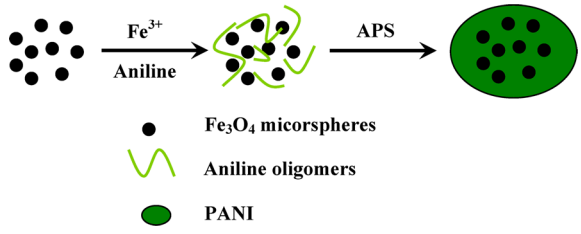

Figure 2. Possible formation mechanism of "egg-like" FMS/PANI.

Although Fe^{3+} and APS are common oxidants for aniline polymerization, weak acidic medium (ca. 0.02 M HCl) is applied here to avoid the dissolution of Fe_3O_4 microspheres, where Fe^{3+} prefers to induce the formation of aniline oligomers rather than PANI powders. This can be proved by the obvious change of UV/vis spectra (Figure S2, Supporting Information) and rather limited change in the weight of solid product (the yield of PANI is generally less than 10 wt %) as compared to that of initial Fe_3O_4 microspheres if we stop the polymerization before adding APS. These aniline oligomers surrounding Fe_3O_4 microspheres will be further polymerized into PANI by the addition of APS. When the content of aniline increases, the

dx.doi.org/10.1021/jp3024099 | J. Phys. Chem. B 2012, 116, 9523−9531

resultant PANI gradually assembles into "egg-like" aggregates and traps most of Fe_3O_4 microspheres (Figure 1). In contrast, in the synthesis of OO-FMS/$PANI_{50}$, aniline monomers are directly oxidized into PANI without prepolymerization. Some PANI grows at the surface of Fe_3O_4 microspheres, and the rest is just randomly polymerized in the solution, thus leading to the disordered microstructure.

The addition of APS results in an increase of PANI yield, but still not all aniline monomers can be transformed into PANI due to the weak acidic medium. For all FMS/PANI composites, the total weights of Fe_3O_4 microspheres and aniline monomers in initial solution are fixed at 2.0 g, but we only get 1.90, 1.73, 1.67, 1.60, 1.58, and 1.54 g for FMS/$PANI_{10}$, FMS/$PANI_{30}$, FMS/$PANI_{50}$, FMS-$PANI_{70}$, FMS-$PANI_{90}$, and FMS-$PANI_{100}$, respectively. Considering that the dissolution of Fe_3O_4 microspheres in the current state is negligible, one can estimate the theoretical PANI contents in these composites as 5.3%, 19.1%, 40.1%, 62.5%, 87.3%, and 100%, respectively. The thermogravimetric (TG) measurement is used to verify the theoretical estimation of PANI contents by taking FMS/$PANI_{50}$ as a random sample, as shown in Figure S3 (Supporting Information). Two weight-loss steps can be observed: the first one below 150 °C due to the removal of surface-absorbed water, and the second one between 150 and 500 °C arising from the combustion of PANI. Deducting the surface-absorbed water and oxidation transformation from Fe_3O_4 to Fe_2O_3, the PANI content in FMS/$PANI_{50}$ is about 41.8 wt %, which is very close to the theoretical content (40.1 wt %). In addition, the TG curves of OO-FMS/$PANI_{50}$, FNP/$PANI_{50}$, and PM-FMS/PANI are shown in Figure S4 (Supporting Information), and their PANI contents calculated by the same method are 43.7%, 39.7%, and 40.0%, respectively, close to that of FMS/$PANI_{50}$. Therefore, it is reliable and meaningful to compare their differences in electromagnetic properties and microwave absorption under the same conditions.

Figure 3 shows the FT-IR spectra of FMS/PANI composites with different mass contents of PANI. For Fe_3O_4 microspheres (FMS/$PANI_0$), one peak at 580 cm^{-1} indexed to Fe−O vibration can be observed. Additional peaks in the ranges 1600−1700 and 1000−1100 cm^{-1} can be attributed to H_2O molecules and trace amount of organic residuals. With the increase in the content of aniline monomer, some characteristic peaks of PANI, such as C═C stretching deformations of quinoid (1570 cm^{-1}) and benzenoid rings (1479 cm^{-1}), the C−N stretching of secondary aromatic amine (1295 and 1238 cm^{-1}), the aromatic C−H in-plane bending (1123 cm^{-1}), and the out-of-plane deformation of C−H in the 1,4-disubstituted benzene ring (798 cm^{-1}) can be observed,[29−31] further confirming the presence of PANI in the composites. It is worthwhile to note that there are a few shifts in the wavenumbers of FMS/$PANI_{10}$ and FMS/$PANI_{30}$ as compared to neat PANI, especially at 1570, 1479, and 1123 cm^{-1} (marked by the black arrows), suggestive of the interaction between PANI and Fe_3O_4 microspheres.[32] But in the composites with more PANI, these slight shifts will be overlapped. Very interestingly, UV/vis absorption spectra further enlarge these differences in FMS/$PANI_{10}$ and FMS/$PANI_{30}$, as shown in Figure 4. Neat PANI, FMS/$PANI_{90}$, FMS/$PANI_{70}$, and FMS/

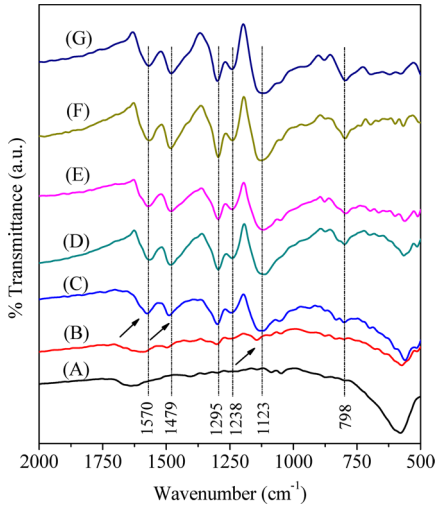

Figure 3. FT-IR spectra of FMS/$PANI_0$ (A), FMS/$PANI_{10}$ (B), FMS/$PANI_{30}$ (C), FMS/$PANI_{50}$ (D), FMS/$PANI_{70}$ (E), FMS/$PANI_{90}$ (F), and FMS/$PANI_{100}$ (G).

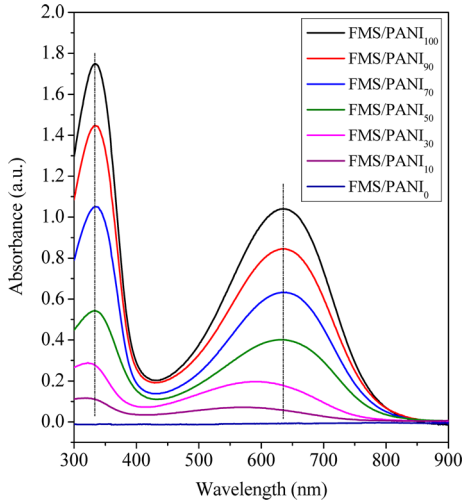

Figure 4. UV/vis spectra of FMS/$PANI_x$.

$PANI_{50}$ exhibit two characteristic bands at about 330 and 635 nm, which can be attributed to the $\pi-\pi^*$ transition of the benzenoid ring and the benzenoid−quinoid excitonic transition, respectively, identical to conventional PANI powders.[32,33] In contrast, the bands corresponding to the benzenoid−quinoid excitonic transition of FMS/$PANI_{30}$ and FMS/$PANI_{10}$ display obvious negative shift, which are located at 591 and 571 nm, respectively. This blue shift may be explained by the increasing energy of the antibonding orbital as a result of the interaction between PANI and Fe_3O_4 microspheres,[34] which agrees well with the results of FT-IR. A similar phenomenon can be also observed in other UV/vis absorption spectra of PANI-based composites.[34−36] In addition, Fe_3O_4, insoluble in *N*-methylpyrrolidone, exhibits no absorption in UV/vis spectra.

The crystalline phases of various composites are clearly characterized by XRD (Figure 5). Fe_3O_4 microspheres exhibit obvious peaks at 30.1°, 35.5°, 43.1°, 53.4°, 57.0°, and 62.6°, which are typically indexed to the crystal phase of Fe_3O_4 (JCPDS 65-3107). From Scherrer's equation,[37] it is estimated that average particle size of Fe_3O_4 is about 20 nm, against the observation in SEM image (Figure 1A), indicating that these Fe_3O_4 microspheres are actually assembled by Fe_3O_4 nanoparticles.[25] When the loadings of PANI increase, the intensities

dx.doi.org/10.1021/jp3024099 | J. Phys. Chem. B 2012, 116, 9523−9531

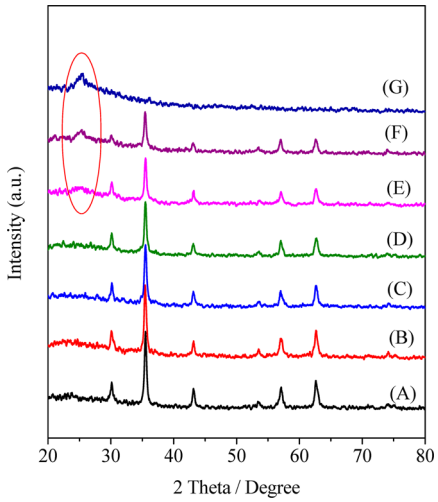

Figure 5. XRD patterns of FMS/PANI$_0$ (A), FMS/PANI$_{10}$ (B), FMS/PANI$_{30}$ (C), FMS/PANI$_{50}$ (D), FMS/PANI$_{70}$ (E), FMS/PANI$_{90}$ (F), and FMS/PANI$_{100}$ (G).

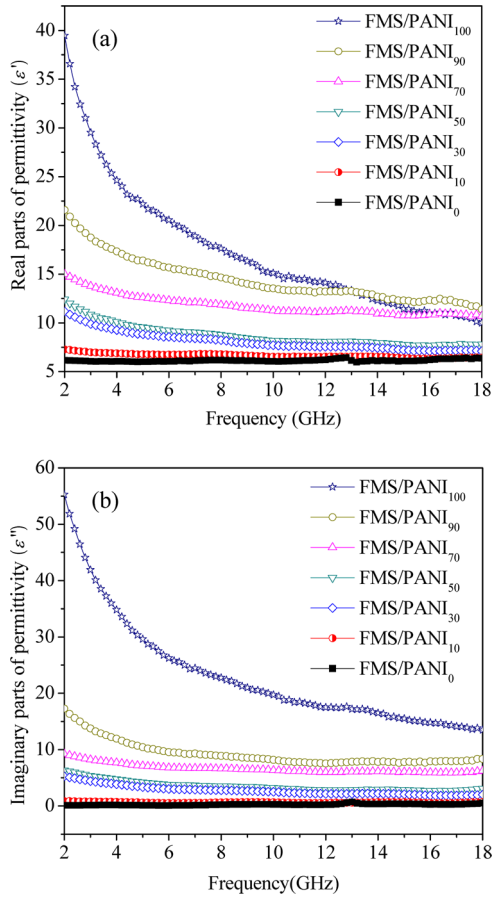

Figure 6. Real parts (a) and imaginary parts (b) of the complex permittivity of FMS/PANI composites in the frequency range 2−18 GHz.

of the diffraction peaks associated with Fe_3O_4 become weaker, and a new broad peak at about 25.4° assigned to the (200) plane of PANI appears when the aniline content reaches 70%, implying that the PANI in these composites is poorly crystallized.[38] By considering almost the same XRD patterns of Fe_3O_4 and γ-Fe_2O_3, XPS measurement is carried out to unambiguously assign the crystal phase by taking FMS/PANI$_{50}$ as a random sample (Figure S5, Supporting Information). The peaks generally shift to higher binding energy and become broader for Fe_3O_4 due to the appearance of Fe^{2+} ($2p_{3/2}$) and Fe^{2+} ($2p_{1/2}$), whereas the presence of the satellite peak at around 719.2 eV is characteristic of γ-Fe_2O_3.[24,39] In our case, the signals are less resolved due to the presence of PANI on the external surface of microspheres; thus it is difficult to distinguish the satellite peak at around 719.2 eV. However, the extremely high binding energies of Fe $2p_{3/2}$ and Fe $2p_{1/2}$ located at 711.6 and 725.6 eV, respectively, indicate that the inorganic phase in these composites is still Fe_3O_4 rather than γ-Fe_2O_3.

It is well-known that microwave absorption properties of a absorber are highly associated with its complex permittivity and complex permeability, where the real parts of complex permittivity (ε') and complex permeability (μ') represent the storage capability of electric and magnetic energy, and imaginary parts (ε'' and μ'') represent the loss capability of electric and magnetic energy.[18,40] Figure 6 shows the ε' and ε'' of all FMS/PANI composites in the frequency range 2−18 GHz. The ε' and ε'' of Fe_3O_4 microspheres are almost constant throughout the whole frequency range except for a very weak resonance behavior at about 13.0 GHz. ε'' values are very close to zero, indicating very poor dielectric loss of Fe_3O_4 microspheres. With increasing content of PANI, both ε' and ε'' are obviously enhanced and become more and more dependent on the frequency. For example, the ε' values of FMS/PANI$_{10}$, FMS/PANI$_{30}$, FMS/PANI$_{50}$, FMS/PANI$_{70}$, FMS/PANI$_{90}$, and FMS/PANI$_{100}$ decrease from 7.28 to 6.44, 11.18 to 7.1, 12.41 to 7.8, 15.03 to 10.71, 21.58 to 11.39, and 39.47 to 10.0, respectively; the ε'' values of FMS/PANI$_{30}$, FMS/PANI$_{50}$, FMS/PANI$_{70}$, FMS/PANI$_{90}$, and FMS/PANI$_{100}$ decline from 5.27 to 2.01, 6.35 to 3.07, 9.27 to 6.25, 17.29 to 8.36, and 55.25 to 13.49, respectively. ε'' of FMS/PANI$_{10}$ has negligible variation, just like that of Fe_3O_4, because of its considerably low content of PANI. These phenomena may be explained by two aspects: (1) PANI has high electrical conductivities; thus strong polarization will occur due to the presence of polaron/bipolaron and other bound charges, which leads to the improvement in ε' and ε''. With the increase in frequency, the dipoles present in the system cannot reorient themselves along with the applied electric field, resulting in decreases in dielectric constant.; (2) The incremental content of PANI results in almost complete coating on Fe_3O_4 microspheres, so that the core/shell microstructure will also contribute to the improvement in ε' and ε'' due to additional interfacial polarization at the surface of microspheres.[5,41] All results indicate that PANI plays a dominant role in determining the dielectric loss properties of these composites.

Figure 7 shows the μ' and μ'' of all FMS/PANI composites in the frequency range 2−18 GHz, where the μ' value of Fe_3O_4 microspheres exhibits an abrupt decrease from 1.42 to 0.83 in the range 2−8.4 GHz and then increases to 0.94 and retains an approximate constant over 10−18 GHz, implying a normal resonance phenomenon. FMS/PANI$_{10}$ displays a variation in μ' values quite similar to that of Fe_3O_4 microspheres because of its low PANI content. It is interesting to discover that the FMS/PANI composites with more PANI give higher μ' values at relatively high frequencies, particularly in the range 4.8−10 GHz, whereas inverse changes are distinguished over 2−4 GHz. Meanwhile, the μ'' of Fe_3O_4 microspheres shows a broad band in the range 2−10 GHz and keeps almost constant near zero in

dx.doi.org/10.1021/jp3024099 | J. Phys. Chem. B 2012, 116, 9523−9531

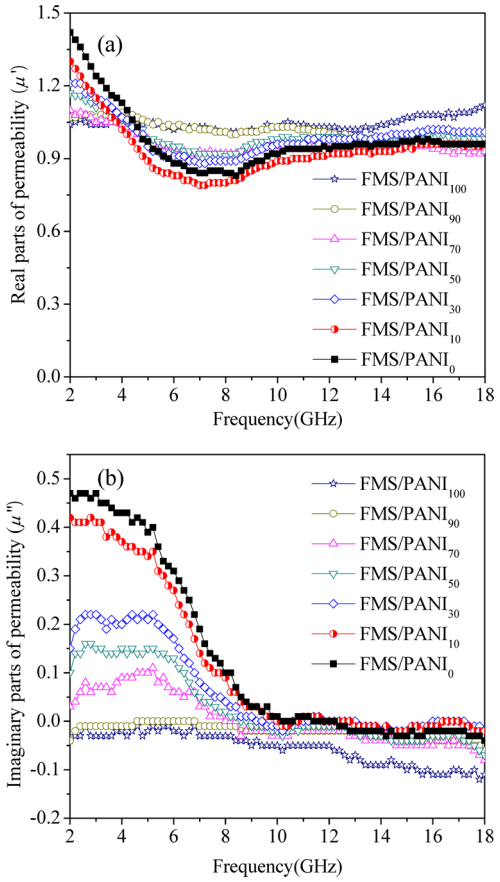

Figure 7. Real parts (a) and imaginary parts (b) of the complex permeability of FMS/PANI composites in the frequency range 2−18 GHz.

the range 10−18 GHz, confirming that Fe_3O_4 microspheres herein break through the Snoek's limit and possess a natural resonance in GHz frequency ranges. The μ'' values of FMS/PANI composites are uniformly smaller than that of Fe_3O_4 microspheres in the response ranges with the increase in PANI content, until the content of aniline monomers reaches 90%, the natural resonance behavior disappears. This indicates that embedding Fe_3O_4 microspheres in a PANI matrix will produce magnetic natural resonance and magnetic loss abilities in the composites, which are highly dependent on the content of Fe_3O_4 microspheres. It can be expected that the derived magnetic loss together with dielectric loss will bring effective enhancement in the reflection loss of incident electromagnetic waves.

On the basis of the measured data of the complex permittivity and complex permeability (Figure 6 and 7), the reflection loss properties (R(dB)) of FMS/PANI composites can be deduced from the transmission line theory,

$$R\ (\mathrm{dB}) = 20 \log \left| \frac{Z_{\mathrm{in}} - 1}{Z_{\mathrm{in}} + 1} \right| \tag{1}$$

Z_{in} refers to the normalized input impedance of a metal-backed microwave absorbing layer and is given by[42,43]

$$Z_{\mathrm{in}} = \sqrt{\frac{\mu_{\mathrm{r}}}{\varepsilon_{\mathrm{r}}}} \tanh\left[j\left(\frac{2\pi}{c}\right) fd\sqrt{\mu_{\mathrm{r}}\varepsilon_{\mathrm{r}}} \right] \tag{2}$$

where ε_{r} ($\varepsilon_{\mathrm{r}} = \varepsilon' - j\varepsilon''$) and μ_{r} ($\mu_{\mathrm{r}} = \mu' - j\mu''$) are the complex permittivity and permeability respectively, of the composite medium, c is the velocity of electromagnetic waves in free space, f is the frequency of microwave, and d is the thickness of an absorber. Figure 8 shows the calculated reflection loss curves of

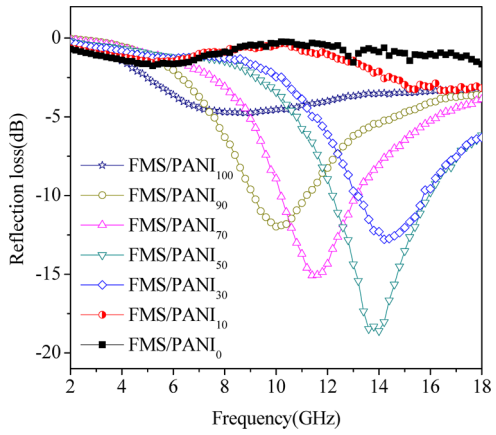

Figure 8. Reflection loss curves of FMS/PANI composites with an absorber thickness of 2 mm in the frequency range 2−18 GHz.

FMS/PANI composites with a thickness of 2 mm in the frequency range 2−18 GHz. It can be seen that the reflection loss properties are sensitive to the content of PANI in the composites. Fe_3O_4 microspheres (FMS/$PANI_0$) and FMS/$PANI_{10}$ exhibit distinguishable magnetic loss abilities, but they still fail to produce considerable reflection loss characteristics, which are less than −5 dB in the whole frequency range due to their very poor dielectric loss (Figure 6). It can be observed that the reflection loss properties toward incident electromagnetic waves of FMS/PANI composites are enhanced substantially with a further increase in the content of PANI, and the frequency relating to the maximum reflection loss can be modulated by the content of PANI in the composites. The maximum reflection losses of FMS/$PANI_{30}$, FMS/$PANI_{50}$, FMS/$PANI_{70}$, and FMS/$PANI_{90}$ are −12.8, −18.6, −15.1, and −12.0 dB at 14.2, 14.0, 11.4, and 10.0 GHz, respectively, and the bandwidths exceeding −10 dB (90% absorption) for these composites are 13.1−15.8, 12.1−16.0, 10.2−13.1, and 9.1−11.1 GHz. Of note is that neat PANI (FMS/$PANI_{100}$) only displays a maximum reflection loss less than −5 dB at 8.8 GHz, although it has larger ε' and ε'' than other composites. As mentioned above, another important parameter relating to reflection loss is the concept of matched characteristic impedance, where the characteristic impedance of the absorbing materials should be equal/close to that of the free space (377 Ω sq^{-1}) to achieve zero-reflection at the front surface of the materials.[3] An overlarge difference between the complex permittivity and complex permeability of PANI cannot bring considerable microwave absorption, because most of electromagnetic waves are reflected off at its surface.[40,44] Enhancement in microwave absorption of FMS/$PANI_{30}$, FMS/$PANI_{50}$, FMS/$PANI_{70}$, and FMS/$PANI_{90}$ can be explained as follows. Embedding Fe_3O_4 microspheres effectively decreases the complex permittivity and increases the complex permeability, leading to improved characteristic impedances and magnetic loss abilities. Moreover, the consequent core/shell interfaces will produce interfacial relaxation between Fe_3O_4 microspheres and PANI, which is also beneficial to microwave absorption according to previous papers.[45,46] Considering the

dx.doi.org/10.1021/jp3024099 | J. Phys. Chem. B 2012, 116, 9523−9531

maximum reflection loss and response bandwidth, FMS/$PANI_{50}$ can be taken as a prominent example of synergetic behavior between Fe_3O_4 microspheres and PANI.

To prove the advantages of Fe_3O_4 microspheres and the two-step oxidation polymerization, the microwave absorption of PM-FMS/PANI, FNP/$PANI_{50}$, and OO-FMS/$PANI_{50}$ are compared in Figure 9. Compared with FMS/$PANI_{50}$, the

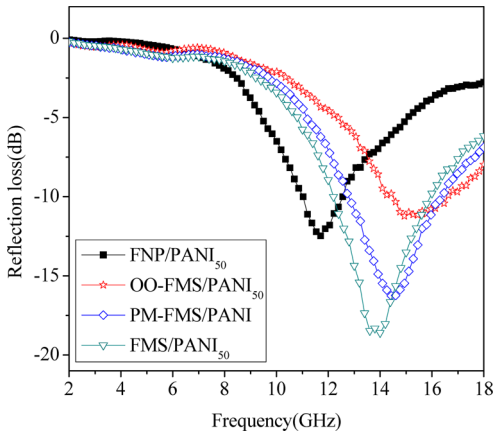

Figure 9. Reflection loss curves of various composites with an absorber thickness of 2 mm in the frequency range 2−18 GHz.

maximum reflection loss of PM-FMS/PANI is more or less attenuated and the corresponding frequency shifts from 14.0 to 14.4 GHz, whereas the attenuation in reflection loss becomes deteriorative in FNP/$PANI_{50}$ and OO-FMS/$PANI_{50}$, whose maxima are only −12.5 dB at 11.7 GHz and −11.2 dB at 14.9 GHz. Considering the approximately same content of ferrite in these composites, it is interesting to find out the key point that induces the difference in reflection loss properties by analyzing the complex permittivity and complex permeability (Figure S6, Supporting Information). As observed, PM-FMS/PANI shows electromagnetic parameters quite similar to those of FMS/$PANI_{50}$ except for a relatively small ε'', indicating that the dielectric loss ability of PM-FMS/PANI is less than that of FMS/$PANI_{50}$; thus PM-FMS/PANI displays a slight decrease in reflection loss. In addition, it can be also found that there are a lot of Fe_3O_4 microspheres on the external surface of PM-FMS/PANI, and most of them are wrapped by PANI in FMS/$PANI_{50}$. This inverse microstructure in PM-FMS/PANI results in its very poor corrosion resistance to acidic environment (Figure S7, Supporting Information), which is not qualified as a promising microwave absorber. As expected, FNP/$PANI_{50}$ from Fe_3O_4 nanoparticles is incapable of magnetic loss as proved by the μ' and μ'' close to 1 and 0, respectively, because of Snoek's limit for Fe_3O_4 nanoparticles. It is also important to note that FNP/$PANI_{50}$ exhibits an increase in the value of ε' and a decrease in ε'' compared with FMS/$PANI_{50}$, indicating the dielectric loss ability of FNP/$PANI_{50}$ is also attenuated to a certain degree. FMS/$PANI_{50}$ and FNP/$PANI_{50}$ have similar microstructures and Fe_3O_4 contents; thus Fe_3O_4 microspheres in these composites are more than just the source of magnetic loss, which can also affect the complex permititvity by the interaction with PANI and improve dielectric loss ability of these composites. Although OO-FMS/$PANI_{50}$ is also prepared from Fe_3O_4 microspheres and gives μ' and μ'' quite similar to those of FMS/$PANI_{50}$, it still fails in showing comparable reflection loss, because the ε' and ε'' of OO-FMS/$PANI_{50}$ are clearly smaller than those of FMS/$PANI_{50}$. It is generally accepted that the complex permittivity is associated with the electrical conductivity, and high electrical conductivity is prone to produce high complex permittivity.[46] According to a previous literature,[38] PANI oxidized by Fe^{3+} favors higher conductivity than that oxidized by APS. Therefore, it is not surprising that FMS/$PANI_{50}$ prepared by two-step oxidation with Fe^{3+} and APS exhibits larger ε' and ε'' than OO-FMS/$PANI_{50}$ prepared with only APS. In other words, two-step chemical oxidation is beneficial to retain considerable dielectric loss in these composites after involving a large amount of Fe_3O_4 microspheres.

According to eq 2, the thickness (d) of absorbers can also affect the reflection loss; thus, the relationship between the thickness and the reflection loss of FMS/$PANI_{50}$ is investigated in Figure 10. The microwave frequency corresponding to the

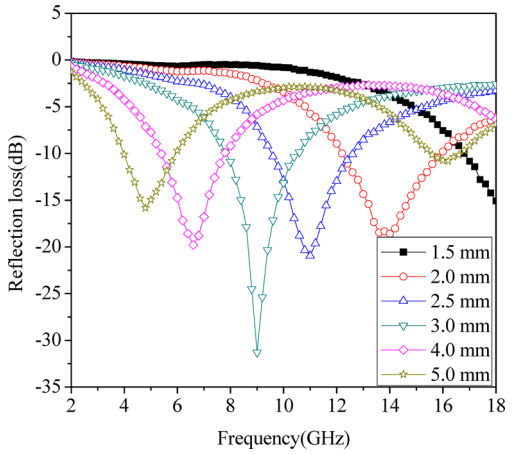

Figure 10. Reflection loss curves dependent on the thickness of FMS/$PANI_{50}$ in the frequency range 2−18 GHz.

maximum reflection loss shifts negatively with the increase of thickness, and the value of reflection loss exceeding −10 dB can be obtained in the range 4.0−18 GHz with a variation in thickness from 1.5 to 5.0 mm. Besides, a maximum of −31.3 dB at 9 GHz can be achieved when the thickness is 3.0 mm. The strong reflection loss over such wide frequency ranges in FMS/$PANI_{50}$ is superior to some of the best ever reported composites of Fe_3O_4 nanoparticles and conductive polymers.[13−18] We believe that FMS/$PANI_{50}$ will be a promising microwave absorber, whose absorption band can be simply modulated by manipulating the thickness to satisfy the applications in different frequency bands.

4. CONCLUSION

We demonstrate here for the first time synthesis of composites consisting of Fe_3O_4 microspheres and PANI by a novel two-step oxidative polymerization method, with Fe^{3+} and APS as oxidants. It can be inferred by SEM, mass analysis, and UV/vis spectra that Fe^{3+} induces the formation of aniline oligomers in the first stage, and APS stimulates the formation of PANI in the second stage. The two-step chemical oxidation is responsible for the "egg-like" morphology of these composites. The results of XRD and XPS suggest that Fe_3O_4 microspheres in these composites have not been oxidized by APS during the polymerization of aniline. FT-IR and UV/vis spectra reveal the interaction between Fe_3O_4 microspheres and PANI in the composites. More importantly, it can be found that embedding Fe_3O_4 microspheres will not only modulate the complex

dx.doi.org/10.1021/jp3024099 | J. Phys. Chem. B 2012, 116, 9523−9531

permittivity but also produce magnetic resonance and loss in the composites. As a result, the characteristic impedance and reflection loss of these composites are strongly improved. By investigating the electromagnetic properties and reflection loss characteristics of other composites from Fe_3O_4 nanoparticles (FNP/PANI), one-step oxidation (OO-FMS/PANI), and physical mixture (PM-FMS/PANI), it is easy to conclude the advantages of Fe_3O_4 microspheres and two-step oxidation polymerization as follows: (1) Fe_3O_4 microspheres can produce magnetic resonance and loss in the composites, which are incapable to general Fe_3O_4 nanoparticles; (2) Fe_3O_4 microspheres exhibit better performance in modulating the complex permittivity than general Fe_3O_4 nanoparticles, leading to a superior dielectric loss; (3) two-step chemical oxidation including prepolymerization induced by Fe^{3+} is beneficial to retain better dielectric loss than one-step chemical oxidation by APS; (4) the composites from two-step chemical oxidation favor considerable environmental stability, because most of Fe_3O_4 microspheres have been completely coated by PANI. In view of the results in this article, we believe that the two-step chemical oxidative polymerization may be a proper route for constructing lightweight and highly effective microwave absorbing composites with hierarchically magnetic materials and conductive polymers.

■ ASSOCIATED CONTENT

Ⓢ Supporting Information

SEM images, TG curves, complex permittivity, and complex permeability of $FMS/PANI_{50}$, $FNP/PANI_{50}$, $OO\text{-}FMS/PANI_{50}$, and PM-FMS/PANI; Photograph and UV/vis absorption spectra of initial solution and filtrate catalyzed with only Fe^{3+}; XPS and anticorrosion photograph of $FMS/PANI_{50}$. This material is available free of charge via the Internet at http://pubs.acs.org.

■ AUTHOR INFORMATION

Corresponding Author

*Fax: +86-(451)-86418750. Tel: +86-(451)-86413702. E-mail: Y.D., yunchendu@yahoo.com.cn; P.X., pxu@hit.edu.cn.

Notes

The authors declare no competing financial interest.

■ ACKNOWLEDGMENTS

This work is supported by National Natural Science Foundation of China (21003029, 21071037, 21101041 and 91122002), Special Fund of Harbin Technological Innovation (2010RFXXG012), Postdoctoral Science-research Development Foundation of Heilongjiang Province (LBH-Q11098), and Fundamental Research Funds for the Central Universities (Grant No. HIT.NSRIF.2010065, HIT.NSRIF.2011017, and HIT.BRETIII.201223).

■ REFERENCES

(1) Olmedo, L.; Hourquebie, P.; Jousse, F. *Adv. Mater.* **1993**, *5*, 373–377.
(2) Chandrasekhar, P.; Naishadham, K. *Synth. Met.* **1999**, *105*, 115–120.
(3) Vinoy, K. J.; Jha, R. M. *Radar Absorbing Materials: From Theory to Design and Characterization*; Kluwer: Boston, 1996.
(4) Xu, P.; Han, X. J.; Wang, C.; Zhao, H. T.; Wang, J. Y.; Wang, X. H.; Zhang, B. *J. Phys. Chem. B* **2008**, *112*, 2775–2781.
(5) Ohlan, A.; Singh, K.; Chandra, A.; Dhawan, S. K. *ACS Appl. Mater. Int.* **2010**, *2*, 927–933.
(6) Du, L.; Du, Y. C.; Li, Y.; Wang, J. Y.; Wang, C.; Wang, X. H.; Xu, P.; Han, X. J. *J. Phys. Chem. C* **2010**, *114*, 19600–19606.
(7) Hosseini, S. H.; Mohseni, S. H.; Asadniac, A.; Kerdari, H. *J. Alloy. Compd.* **2011**, *509*, 4682–4687.
(8) Dong, X. L.; Zhang, X. F.; Zuo, F. *Appl. Phys. Lett.* **2008**, *92*, 013127.
(9) Wang, Z. Z.; Bi, H.; Liu, J.; Sun, T.; Wu, X. L. *J. Magn. Magn. Mater.* **2008**, *320*, 2132–2139.
(10) Xu, P.; Han, X. J.; Jiang, J. J.; Wang, X. H.; Li, X. D.; Wen, A. H. *J. Phys. Chem. C* **2007**, *111*, 12603–12608.
(11) Ohlan, A.; Singh, K.; Chandra, A.; Singh, V. N.; Dhawan, S. K. *J. Appl. Phys.* **2009**, *106*, 044305.
(12) Yang, C. C.; Gung, Y. J.; Hung, W. C.; Ting, T. H.; Wu, K. H. *Compos. Sci. Technol.* **2010**, *70*, 466–471.
(13) He, Z. F.; Fang, Y.; Wang, X. J.; Pang, H. *Synth. Met.* **2011**, *161*, 420–425.
(14) Yang, C. H.; Du, J. J.; Peng, Q.; Qiao, R. R.; Chen, W.; Xu, C. L.; Shuai, Z. G.; Gao, M. Y. *J. Phys. Chem. B* **2009**, *113*, 5052–5058.
(15) Phang, S. W.; Tadokoro, M.; Watanabe, J.; Kuramoto, N. *Polym. Adv. Technol.* **2009**, *20*, 550–557.
(16) Phang, S. W.; Kuramoto, N. *Polym. Composite* **2010**, *31*, 516–523.
(17) Yang, C. M.; Li, H. Y.; Xiong, D. B.; Cao, Z. Y. *React. Funct. Polym.* **2009**, *69*, 137–144.
(18) Li, Y. B.; Chen, G.; Li, Q. H.; Qiu, G. Z.; Liu, X. H. *J. Alloy. Compd.* **2011**, *509*, 4104–4107.
(19) Nakamura, T. *J. Appl. Phys.* **2000**, *88*, 348–353.
(20) Tong, G. X.; Wu, W. H.; Guan, J. G.; Qian, H. S.; Yuan, J. H.; Li, W. *J. Alloy. Compd.* **2011**, *509*, 4320–4326.
(21) Jia, K.; Zhao, R.; Zhong, J. C.; Liu, X. B. *J. Magn. Magn. Mater.* **2010**, *322*, 2167–2171.
(22) Ni, S. B.; Sun, X. L.; Wang, X. H.; Zhou, G.; Yang, F.; Wang, J. M.; He, D. Y. *Mater. Chem. Phys.* **2010**, *124*, 353–358.
(23) Wang, F. L.; Liu, J. R.; Kong, J.; Zhang, Z. K.; Wang, X. Z.; Itoh, M.; Machida, K. I. *J. Mater. Chem.* **2011**, *21*, 4314–4320.
(24) Sun, G. B.; Dong, B. X.; Cao, M. H.; Wei, B. Q.; Hu, C. W. *Chem. Mater.* **2011**, *23*, 1587–1593.
(25) Xu, X. Q.; Deng, C. H.; Gao, M. X.; Yu, W. J.; Yang, P. Y.; Zhang, X. M. *Adv. Mater.* **2006**, *18*, 3289–3293.
(26) Kang, Y. S.; Risbud, S.; Rabolt, J. F.; Stroeve, P. *Chem. Mater.* **1996**, *8*, 2209–2211.
(27) Zhang, X. Y.; Goux, W. J.; Manohar, S. K. *J. Am. Soc. Chem.* **2004**, *126*, 4502–4503.
(28) Zhang, X. Y.; Manohar, S. K. *J. Am. Soc. Chem.* **2004**, *126*, 12714–12715.
(29) Zhang, Y. J.; Lin, Y. W.; Chang, C. C.; Wu, T. M. *Synth. Met.* **2010**, *160*, 1086–1091.
(30) Reddy, K. R.; Lee, K. P.; Gopalan, A. I. *Colloid Surf. A* **2008**, *320*, 49–56.
(31) Zhang, S. L.; Kan, S. Q.; Kan, J. Q. *J. Appl. Polym. Sci.* **2006**, *100*, 946–953.
(32) Deng, J. G.; Ding, X. B.; Zhang, W. C.; Peng, Y. X.; Wang, J. H.; Long, X. P.; Li, P.; Chan, A. S. C. *Polymer* **2002**, *43*, 2179–2184.
(33) Xu, P.; Han, X. J.; Wang, C.; Zhang, B.; Wang, X. H.; Wang, H. L. *Macromol. Rapid Commun.* **2008**, *29*, 1392–1397.
(34) Ma, R. T.; Zhao, H. T.; Zhang, G. *Mater. Res. Bull.* **2010**, *45*, 1064–1068.
(35) Godovsky, D. Y.; Varfolomeev, A. E.; Zaretsky, D. F.; Chandrakanthi, R. L. N.; Kundig, A.; Weder, C.; Caseri, W. *J. Mater. Chem.* **2001**, *11*, 2465–2469.
(36) Khanna, P. K.; Lonkar, S. P.; Subbarao, V. V. V. S.; Jun, K. W. *Mater. Chem. Phys.* **2004**, *87*, 49–52.
(37) Cullity, B. D.; Stock, S. R. *Elements of X-ray Diffraction*, 3rd ed.; Prentice-Hall: Englewood Cliffs, NJ, 2001.
(38) Ding, H. J.; Long, Y. Z.; Shen, J. Y.; Wan, M. X. *J. Phys. Chem. B* **2010**, *114*, 115–119.
(39) Teng, X. W.; Black, D.; Watkins, N. J.; Gao, Y. L.; Yang, H. *Nano Lett.* **2003**, *3*, 261–264.

(40) Du, Y. C.; Wang, J. Y.; Cui, C. K.; Liu, X. R.; Wang, X. H.; Han, X. J. *Synth. Met.* **2010**, *160*, 2191−2196.
(41) Ohlan, A.; Singh, K.; Chandra, A.; Dhawan, S. K. *Appl. Phys. Lett.* **2008**, *93*, 053114.
(42) Kim, S. S.; Jo, S. B.; Gueon, K. I.; Choi, K. K.; Churn, K. S. *IEEE Trans. Magn.* **1991**, *27*, 5462−5464.
(43) Singh, P.; Babbar, V. K.; Razdan, A.; Puri, R. K.; Goel, T. C. *J. Appl. Phys.* **2000**, *87*, 4362−4366.
(44) Xu, P.; Han, X. J.; Liu, X. R.; Zhang, B.; Wang, C.; Wang, X. H. *Mater. Chem. Phys.* **2009**, *114*, 556−560.
(45) Zhang, X. F.; Dong, X. L.; Huang, H.; Liu, Y. Y.; Wang, W. N.; Zhu, X. G.; Lv, B.; Lei, J. P.; Lee, C. G. *Appl. Phys. Lett.* **2006**, *89*, 053115.
(46) Xu, P.; Han, X. J.; Wang, C.; Zhou, D. H.; Lv, Z. S.; Wen, A. H.; Wang, X. H.; Zhang, B. *J. Phys. Chem. B* **2008**, *112*, 10443−10448.